International Journal of Development Mathematics Vol 2 Issue 2 Page No. 174 - 189

INTERNATIONAL JOURNAL OF DEVELOPMENT MATHEMATICS

ISSN: 3026-8656 (Print) | 3026-8699 (Online)

journal homepage: https://ijdm.org.ng/index.php/Journals

Nonlinear Thermal Impact on Arrhenius-Propelled Flow in a Porous Microchannel

Godwin Ojemeri[a*], Emmanuel Omokhuale[b], Mohammed D. Maigemu[a] Idris O. Usman[c] Emmanuel B. Gudu[a] and Jeremiah A. Dazi[a]

[a]College of Sciences, Federal University of Agriculture, Zuru, P. M. B. 28, Kebbi State, Nigeria.

[b]Department of Mathematics, Faculty of Sciences, Federal University Gusau, P. M. B. 1001, Zamfara State, Nigeria

[c]Brilliant Footsteps International Academy, Western Bypass, Sokoto. Nigeria

ARTICLE INFO

Article history:
Received 02 February 2025
Received in revised form 10 May 2025
Accepted 20 June 2025

Keywords:
Nonlinear density variation with temperature (NDT), Arrhenius kinetics, Porous medium, Magnetohydrodynamics (MHD), Superhydrophobic (SHO) Microchannel.

MSC 2020 Subject classification:
76D10, 76W05.

ABSTRACT

There are drawbacks to using linear density variation with temperature (LDT), especially in situations where advanced thermal systems for microfluidic devices require higher thermal energy to maximize and maintain. Thus, this work examines the effects of non-linear density variation with temperature (NDT) on a magnetized flow induced by an Arrhenius-driven fluid in a porous medium-filled superhydrophobic (SHO) microchannel. While the other parallel plate has a no-slip surface (NSS), one of the plates is purposefully altered to have superhydrophobic surface (SHS) properties. The semi-analytical (regular perturbation) approach is used to solve the nonlinear ordinary differential equations. A graphic representation of the actions of the main parameters governing the flow behavior in terms of momentum and energy distributions is provided. The Nusselt number and skin friction have been calculated for both surfaces. Because the current study is supported by a comparison with previous research, it is valid for the limiting case. It was discovered that NDT has a higher fluid flow than LDT. Additionally, it is seen that the introduction of NDT strengthens the shear stress in the microchannel, whilst the presence of a porous media accelerates the fluid velocity. Applications of this research will include solid matrix heat exchangers, geothermal systems, anti-wetting microtechnology, and petrochemical engineering.

1. Introduction

The exploration of electrically conductive liquids, namely plasma, electrolytes, salt water, and liquid metals, is called magnetohydrodynamics (MHD). There are numerous technical and commercial applications for this type of liquid, namely magnetic drug targeting, crystal formation, power generation, reactor cooling, and MHD sensors (Jawad *et al.*, 2021). Hartmann and Lazarus (1937) were the first to conduct an experimental study of modern MHD flow in laboratories. This research laid the groundwork for the creation of numerous MHD devices, including MHD pumps, MHD generators, brakes, flow meters, and geothermal-powered energy extraction. Afterwards, numerous research studies have been published to analyze the effects of MHD free convection along different flow media. In view of this, Onwubuya and Ojemeri (2023) used a homotopy perturbation approach to compare MHD mixed convection with a thermal radiation component in an upright porous channel. Hamza et al. (2023a) utilized the homotopy perturbation approach to describe the effect of hydromagnetic natural convection flow on a chemically reactive fluid subjected to symmetric and asymmetric heating conditions. Jha *et al*. (2023) modeled the buoyancy-induced magnetic field flow of a fluid in an upright plate with a point/line heat sink/source at different channel locations. Saeed and Gul (2021) investigated the hydromagnetic Casson nanofluidic flow for mass and heat transmission via a stretching plate. Reddy *et al*. (2018) investigated the effects of cross-diffusion on non-Newtonian fluid flow over an extended range while using an unequal heat sink/source. The Fehlberg technique was used in this analysis to determine the solution to the

* Corresponding author. Tel.: +2348061676148
E-mail address: godwinojemeri@gmail.com (Godwin Ojemeri)
https://doi.org/10.62054/ijdm/0202.09

modeled problem. The authors looked at how fractional and non-uniform heat interacts with the flow regime. Sravanthi and Gorla (2018) addressed how heat absorption/generation and chemical reactions affect Maxwell magnetized nanofluid flux. The authors used semi-analytical and homotopy analysis approaches to solve the defined model in this case, which involved flow across an extended surface with exponential convection. Ojemeri *et al.* (2023a) investigated the hydromagnetic flux of an electrically conducting non-Newtonian liquid induced by the radiative factor in an upright channel. References such as Rostami *et al*. (2021), Obalalu *et al*. (2021), and Uygun *et al*. (2022) provide additional insight into this occurrence.

A novel field of study that is gaining attention is the investigation of MHD in microchannels with jump temperature and superhydrophobic (SHO) properties. Extreme water repellency, self-cleaning mechanisms, decreased friction, and improved flow are some characteristics of microchannels with SHS. Microchannels with SHS can reduce the impact of water exposure on surfaces and promote self-cleaning behavior, claim Lee *et al*. (2021). Microchannels with SHS were used to make small medical testing devices, control the movement of tiny amounts of liquids, separate oil and water in fluid systems, and improve heat transfer by allowing liquids to flow better. Akhtari and Karimi (2020) opined that SHS applied to microchannels can reduce the pumping power required to initiate fluid flow. Several prominent scholars have made significant contributions to the investigation of various phenomena in microchannels impacted by SHS. To that aim, Hamza et al. (2025) recently explored the importance of dusty fluid in unsteady fractional derivatives in Caputo-Fabrizio (CF) and Atangana-Baleanu in Caputo sense (ABC) in addressing heat transfer problems through a SHO microchannel. Further, Hamza et al. (2024a, 2024b) investigated the effects of electrokinetics on free and mixed convection flows in SHO microchannels, as well as the temperature jump scenario. According to their computer study, the SHS and electrokinetic effects serve to increase fluid velocity in the microchannel. In the realm of MHD, Ojemeri and Onwubuya (2023a) highlighted the importance of magnetized mixed flow with porous media in a slit microchannel. Jha and Gwandu (2018, 2020) investigated fluid flow using a magnetic field in an upstanding slit microchannel with SHS, porous material, and a temperature spike. Sharma et al. (2020) developed a mathematical model that represents pressure-induced flow across a microchannel containing textured SHS and a continuous heat flux. Other relevant studies with varied thermal boundary conditions in the presence of SHS may be found in the following references: Sia *et al*. (2023), Heidarian et al. (2020), and Zhang et al. (2019).

Understanding how mass and energy are distributed is critical to improving the efficiency of chemical processes. The advancement and development of novel and more effective methods, materials, and medicines is heavily reliant on chemical processes. Arrhenius-controlled (exothermic chemical reaction) heat transfer through microchannels and slit microchannels coated with SHO surfaces has recently piqued researchers' interest due to its potential applications in the engineering and chemical industries for heat transfer advancement, biomedical devices, and so on. In this context, Ojemeri et al. (2024) have highlighted the importance of heat-generating/absorbing fluid on Arrhenius-controlled heat flow in an SHO heated microchannel using a regular perturbation approach. Ojemeri and Onwubuya (2023b) investigated mixed convection flow in an SHO microchannel caused by the action of a porous material and a chemically driven heat-absorbing/generating fluid. Later, Ojemeri and Onwubuya (2023c) used the semi-analytic technique to explore the effect of magnetized free flow on the Arrhenius-controlled transfer problem in a microchannel with SHO characteristics and temperature jump condition. Hamza et al. (2023b) employed the homotopy perturbation approach to investigate the effects of an Arrhenius-controlled chemical reaction and Hall current on the hydromagnetic free convection flow of an incompressible fluid along an upstanding microchannel under acceptable boundary conditions. Ojemeri et al. (2023b) examined an exothermic chemical reaction in a vertical microchannel filled with porous media employing HPM. Ojemeri and Hamza (2022) emphasized the significance of Arrhenius-controlled heat-generating/absorbing fluids in a microchannel with velocity slip and temperature jump circumstances.

According to the aforementioned literature, the role of nonlinear density variation with temperature (NDT) caused by Arrhenius-controlled heat flow in porous microchannels coated with SHS under temperature jump circumstances is understudied. As a result, the purpose of this research is to investigate the effect of NDT on free

convection in Arrhenius-driven flow in a microchannel filled with porous media, using the work of Ojemeri and Onwubuya (2023c) as a reference. A semi-analytical approach is used to treat the simulated nonlinear equations. In addition to being crucial for enhancing fluid flow in microchannels, the paper's findings will also be used as a guide for designing sophisticated thermal management systems for microfluidic devices and high-performance uses like steel production in metallurgical industries and cracking in thermal decomposition reactions. The findings of this study may also have applications in chemical and technical processes such as wall-cooled catalytic reactors, groundwater hydrology, and underground coal gasification.

2. Formulation of the Problem

Consider a steady magnetized flow of a fluid moving along two vertical parallel plates influenced by exothermic chemical reaction and nonlinear density with temperature factor. As shown in Figure 1, the wall at $y_0 = 0$ is instigated by the extremely difficult-to-wet known as the SHO effect while the NSS is kept at $y_0 = L$. A magnetic field of intensity B_0 is said to be applied perpendicularly to the two upstanding microchannel plates. All the fluid properties are assumed to be constants. The flow variables are functions of space y only. In view of the present formulation, the following assumptions are further made:

i. The fluid is laminar and fully developed.

ii. Nonlinear Boussinesq approximation is assumed to be incorporated into the Navier-Stoke equations as used in Jha and Gwandu (2019).

iii. The plates are assumed to be heated asymmetrically with one plate maintained at a temperature T_0 while the other plate at a temperature T_h.

iv. Due to this temperature gradient between the plates, it is assumed that natural convection flow occurs in the microchannel.

v. It is also assumed that the fluid is influenced by Arrhenius kinetics.

vi. The fluid is assumed to be affected by nonlinearity variable and porous medium

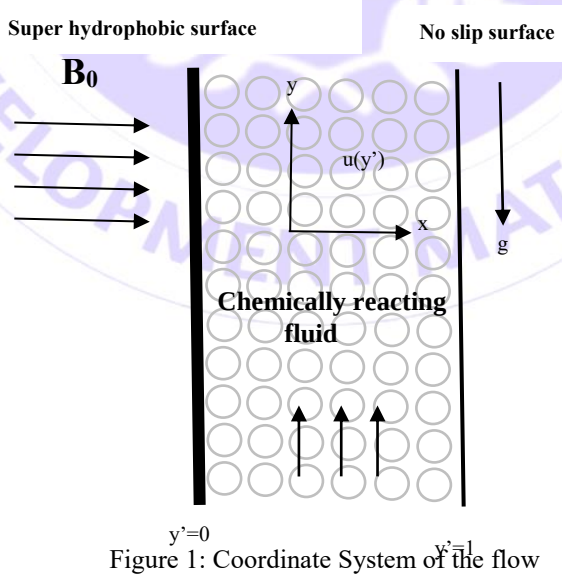

Figure 1: Coordinate System of the flow

Following Ojemeri and Onwubuya (2023c) and Jha and Gwandu (2019), with the appropriate boundary conditions, the dimensional governing equations for the present problem can be expressed as:

$$V\frac{d^2u'}{dz'^2} + g\beta_0(T' - T_O) + g\beta_1(T' - T_O)^2 - \frac{\sigma B_O^2 u'}{\rho} - \frac{u'}{K} = 0 \tag{1}$$

$$\frac{k}{\rho c_\rho}\frac{d^2T'}{dz'^2} + \frac{QC_0^* A}{\rho c_\rho} e^{\left(\frac{-E}{RT'}\right)} = 0 \tag{2}$$

Subject to the boundary conditions:

$$\left.\begin{array}{l} \left.\begin{array}{l} u(z') = \gamma'\frac{du'}{dz'} \\ T(z') = T_h + \Gamma'\frac{dT'}{dz'} \end{array}\right\} at\ z' = 0 \\ \left.\begin{array}{l} u(z') = 0 \\ T(z') = T_o \end{array}\right\} \qquad at\ z' = L \end{array}\right\} \tag{3}$$

Introducing the dimensionless quantities as:

$$u = \frac{u'}{U}, z = \frac{z'}{h}, \theta = \frac{T' - T_0}{T_w - T_o}, x = \frac{x'v}{Uh^2}, M^2 = \frac{\sigma\beta_o^2 h^2}{\rho v}, (Z, \gamma, \Gamma) = (Z', \gamma', \Gamma')/h$$

$$Da = \frac{k}{L^2}, \quad \varepsilon = \frac{RT_0}{E}, \lambda = \frac{QC_0^* AEH^2}{RT_0^2} \tag{4}$$

substituting eqn(4) into eqns (1-3), the basic equations of the temperature and velocity becomes:

$$\frac{d^2U}{dz^2} - M_1^2 U = -\theta - \mathrm{N}\theta^2 \tag{5}$$

$$\frac{d^2\theta}{dz^2} + \lambda e^{\frac{\theta}{1+\varepsilon\theta}} = 0 \tag{6}$$

Restricted to the boundary conditions:

$$\theta(z) = 1 + \Gamma\frac{d\theta}{dz}, \qquad u(z) = \gamma\frac{du}{dz} \qquad \text{at } z = 0 \tag{7}$$

$$\theta(z) = 0, \qquad u(z) = 0 \qquad \text{at } z = 1$$

Where M is the magnetic parameter, N is the nonlinearity parameter, λ is the viscous heating parameter, ε is the activation energy, Γ is the temperature jump parameter, and γ is the velocity slip parameter.

3.0 Method of Solution

The coupled nonlinear governing equations are treated using regular perturbation method such that the solutions of the temperature and velocity is assumed as;

$$U = u_0 + \lambda(u_1) \tag{8}$$

$$T = t_0 + \lambda(t_1) \tag{9}$$

Inserting eqns (8) and (9) into eqns (5) to (7), and taking the coefficients of λ^0 and λ, we derive the following system of ordinary differential equations with their transformed boundary conditions as:

$$\lambda^0: \frac{d^2u_0}{dz^2} - M_1^2 u_0 = -\theta_0 - \mathrm{N}\theta_0^2 \tag{10}$$

$$\lambda: \frac{d^2u_1}{dz^2} - M_1^2 u_1 = -\theta_1 - 2\mathrm{N}\theta_0\theta_1 \tag{11}$$

$$\lambda^0: \frac{d^2\theta_0}{dz^2} = 0 \tag{12}$$

$$\lambda: \frac{d^2\theta_1}{dz^2} + 1 + \theta_0 + (\frac{1}{2} - \varepsilon)\theta_0^2 = 0 \tag{13}$$

$$\left.\begin{array}{l} \lambda^0: \theta_o = 1 + \Gamma\frac{d\theta_o}{dz} \\ \lambda: \theta_1 = \Gamma\frac{d\theta_1}{dz} \\ \lambda^0: u_0 = \gamma\frac{dU_o}{dz} \\ \lambda: u_1 = \gamma\frac{dU_1}{dz} \end{array}\right\} \text{at } z = 0 \tag{14}$$

and

$$\left.\begin{array}{l} \lambda^0: \theta_0 = 0 \\ \lambda: \theta_1 = 0 \\ \lambda^0: u_0 = 0 \\ \lambda: u_1 = 0 \end{array}\right\} \text{at } z = 1 \tag{15}$$

The solutions of temperature and velocity is derived as:

$$\theta_0 = R_1 z + R_2 \tag{16}$$

$$\theta_1 = -\frac{z^2}{2} - R_1\frac{z^6}{3} - R_2\frac{z^2}{2} - e_1(R_1^2\frac{z^4}{12} + R_1R_2\frac{z^3}{3} + R_2^2\frac{z^2}{2} + R_3 z + R_4) \tag{17}$$

$$u_0 = R_5\cosh(M_1 z) + R_6 sinh(M_1 z) + R_2 z^2 + R_8 z + R_9 \tag{18}$$

$$u_1 = R_{10}\cosh(M_1 z) + R_{11} sinh(M_1 z) + R_{12}z^5 + R_{13}z^4 + R_{14}z^3 + R_{15}z^2 + R_{16}z + R_{17} \tag{19}$$

Where the heat transfer rate and shearing stress is derived as:

$$\frac{d\theta}{dz}\Big|_{z=0} = R_1 + \lambda R_3 \tag{20}$$

$$\frac{d\theta}{dz}\Big|_{z=1} = R_1 + \lambda\Big[-z - 2R_1 - 2R_2 - e_1\left(\frac{R_1^2}{3} + R_1R_2 + R_2^2 + R_3\right)\Big] \tag{21}$$

$$\frac{dU}{dz}\Big|_{z=0} = M_1R_6 + R_8 + \lambda[M_1R_{11} + R_{16}] \tag{22}$$

$$\frac{dU}{dz}\Big|_{z=1} = M_1R_5\sinh(M_1) + M_1R_6\cosh(M_1) + R_8 + \lambda[M_1R_{10}\sinh(M_1) + M_1R_{11}\cosh(M_1) + 5R_{12} + 4R_{13} + 3R_{14} + 2R_{15} + R_{16}] \tag{23}$$

Where all the constants used are indicated in the appendix

4.0 Results and Discussion

The significance of the nonlinear thermal effect over the linear one is illustrated in this study. The interaction of Arrhenius-driven heat transfer flow with NDT impact over a porous microchannel coated with SHS and temperature jump characteristics. A semi-analytical method is employed to treat the resultant steady ordinary differential equations. Some analysis graphs have been plotted using MATLAB software to demonstrate the effect of pertinent parameters. The default values chosen for this study are $\gamma = \Gamma = Da = N = 1$, $M = 0.5$, and $\lambda = 0.001$.

Figure 2 shows how the Darcy porosity parameter affects the velocity distribution. It is clear that as the porosity parameter increases, the fluid's velocity grows. We also see that as the permeability of the porous medium increase, the sheer stress decrease, which consequently improves the fluid's velocity profile. This makes practical sense given that moving a large amount of fluid generates more viscous energy, which increase the fluid's thickness as well as promotes the velocity of the fluid. Figure 3 depicts the impact of N on the velocity gradient. The figure shows how a higher level of N increases the fluid's velocity. This is because N increases the temperature, which accelerates the kinetic energy, and, as a result, the velocity increases. This result supports the findings of Jha and Gwandu (2019). Figure 4 depicts the pattern of fluid velocity for different values of the magnetic parameter M. The flow pattern clearly shows a reduction for all investigated M values. The primary cause of this behavior is the presence of a magnetic influence that produces an opposing force (the Lorentz force) that restricts velocity.

Figure 5 depicts the fluctuation of the velocity gradient vs. displacement z, and the findings are consistent with earlier research. This image shows that as particles move away from the SHS, their velocity briefly increases before weakening as they approach the middle. Furthermore, in the absence of SHS and NSS, the fluid's velocity grows slowly before steadily moving until it reaches the microchannel's midpoint. Overall, in the presence of velocity slip and temperature jump, maximum velocity is achieved. Figure 6 shows the deviations of the chemical parameter λ on the temperature gradient. It's worth noting that increasing the value of λ leads to significant temperature improvements. Hamza (2016) found that larger amounts of λ, the chemical reactant parameter, result in a more viscous heating effect, which increases temperature. Similarly, λ increases fluid velocity in the microchannel, as illustrated in Figure 7. Furthermore, it is shown that the fluid surface impact decreases when velocity slip increases at the SHO walls. As a result, the gas flows quicker toward the wall. Higher temperature leads to decreased fluid viscosity and higher flow. Figures 8a and 8b show the function of N versus the skin friction coefficient. It was discovered that increasing N values improves frictional force at the wall (but opposite behavior is observed at the upper plate). Figures 9a and b show how both upstanding walls affect skin friction. When the wall is at y=0, the skin friction is significantly strengthened, as shown in Figure 9a; however, when y=1, the opposite effect occurs, as shown in Figure 9b. Figures 10a and b show the shear stress response favoring the Darcy porous parameter vs. velocity slip at the microchannel walls ($y = 0$ and $y = 1$). These figures show that skin friction decreases as Da increases, whereas the reverse effect occurs at the upper plate.

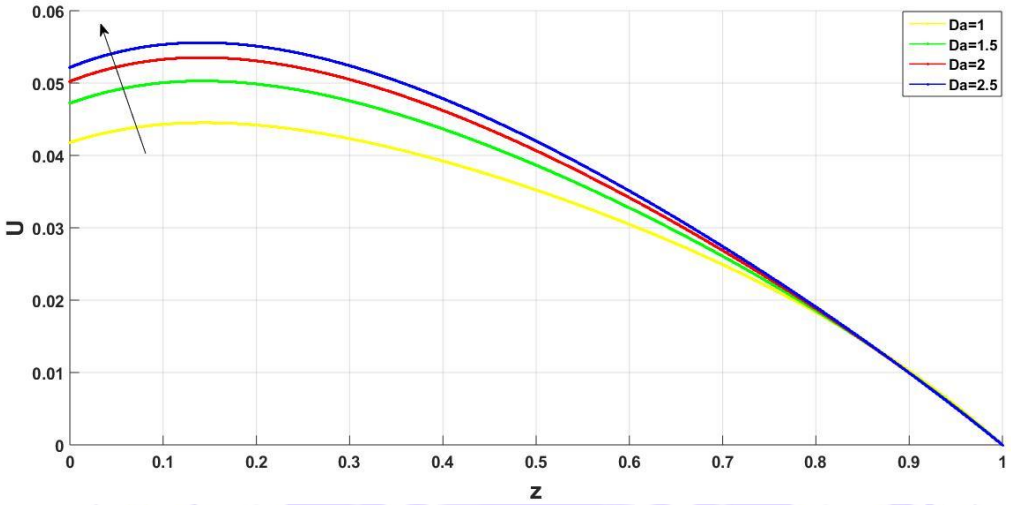

Figure 2: Effect of Da on velocity Gradient

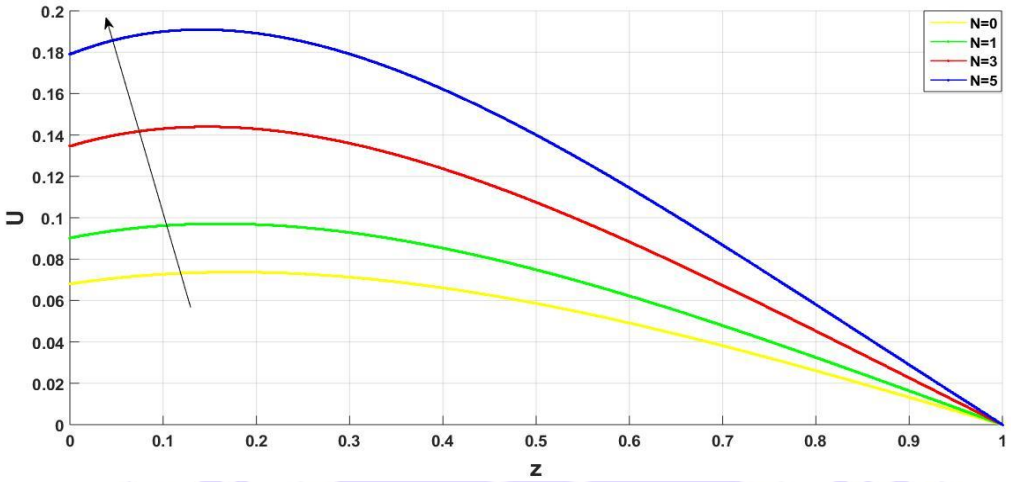

Figure 3: Effect of N on velocity Gradient

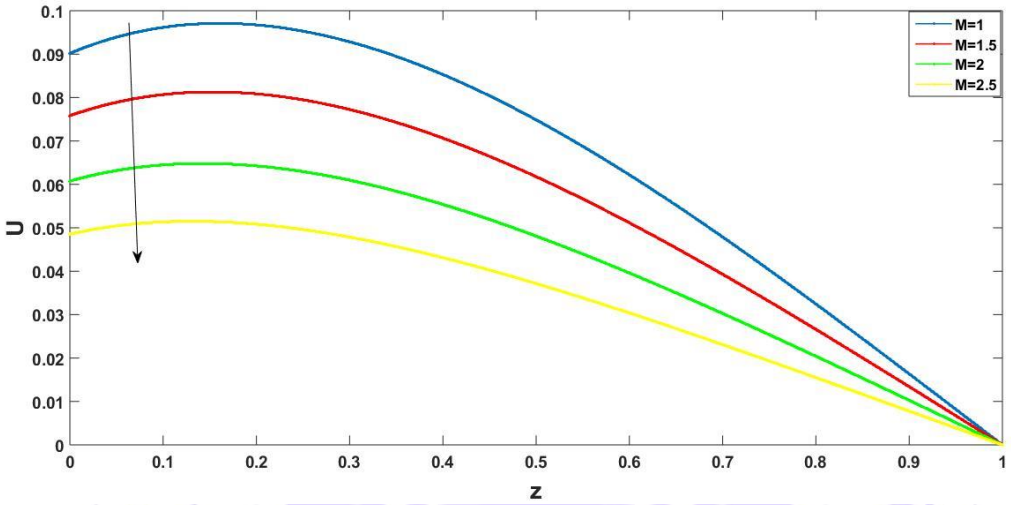

Figure 4: Effect of M on velocity Gradient

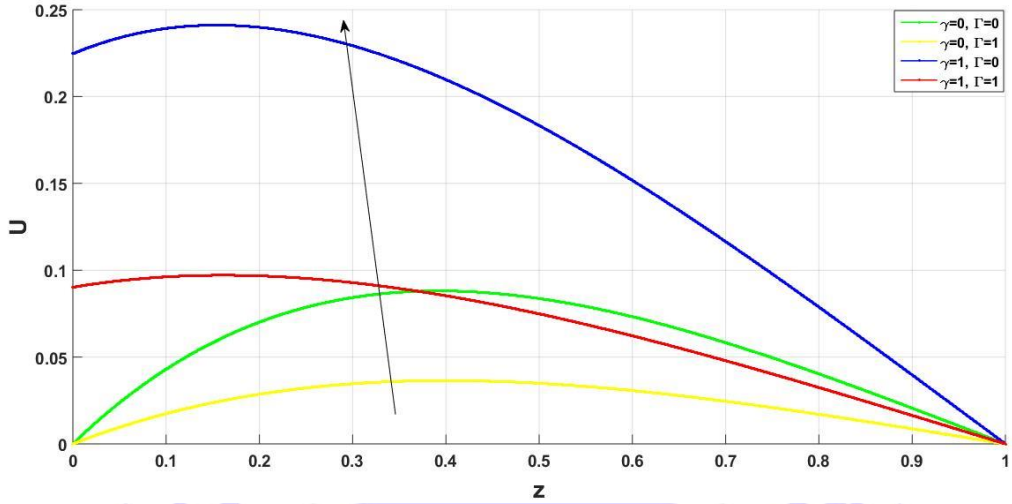

Figure 5: Effect of displacement z on velocity Gradient

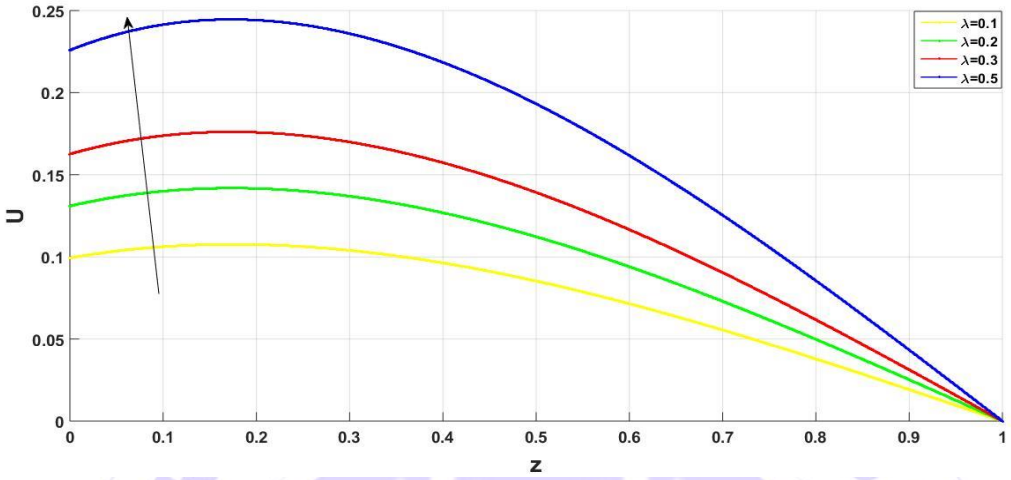

Figure 6: Effect of λ on velocity Gradient

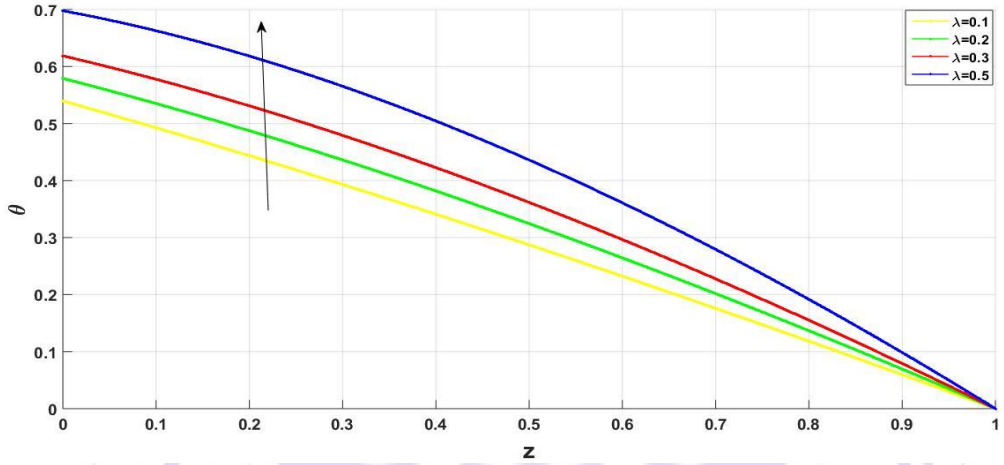

Figure 7: Effect of λ on Temperature Gradient

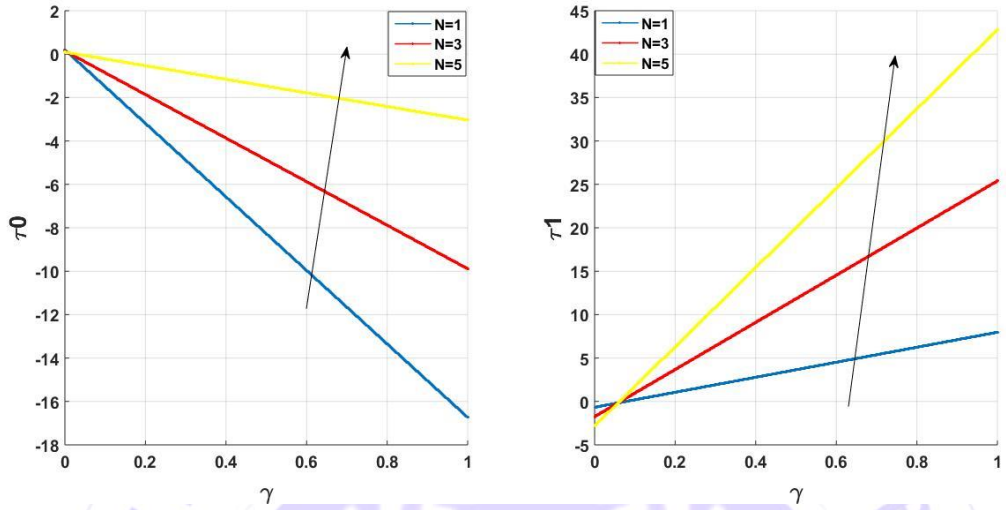

Figure 8: Effect of N on Skin Friction Coefficient

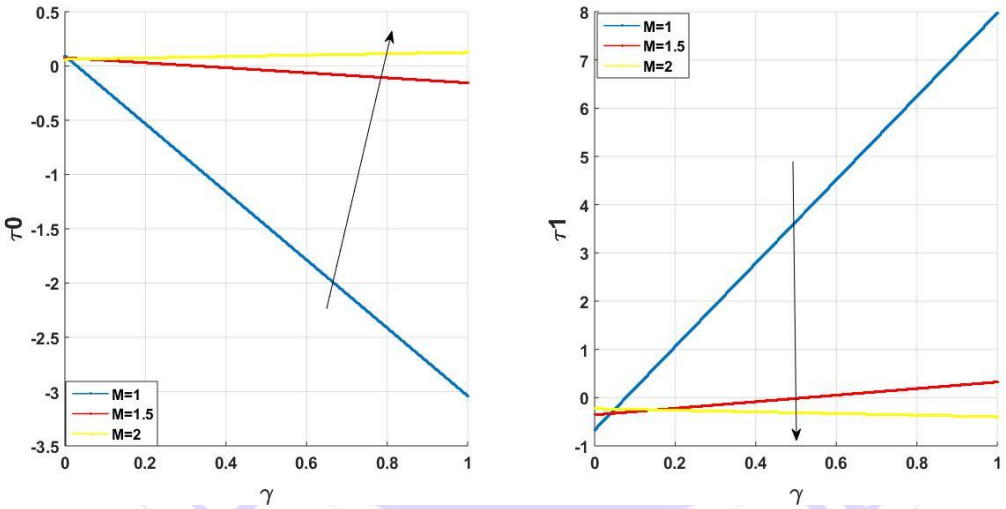

Figure 9: Effect of M on Skin Friction Coefficient

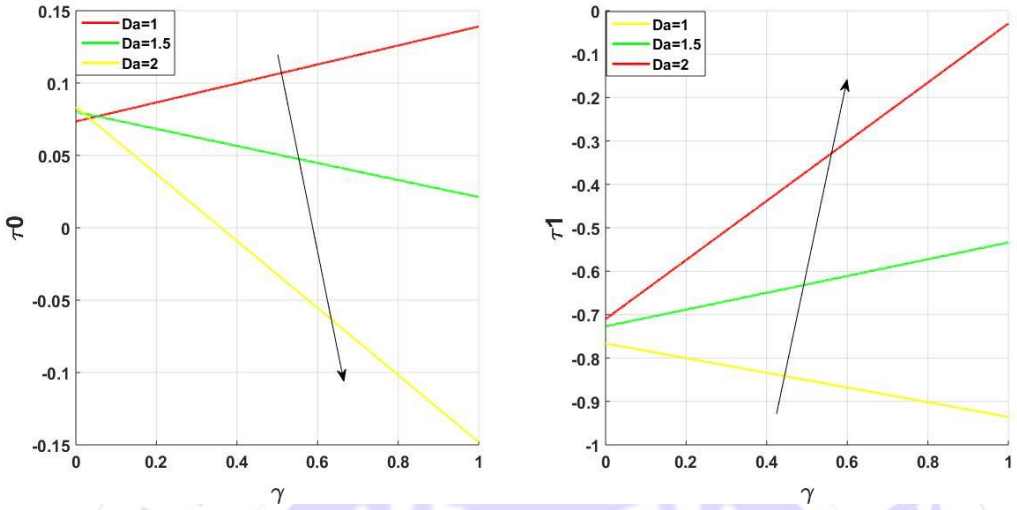

Figure 10: Effect of Da on Skin Friction Coefficient

4.1 Validation of Results

Table 1 is constructed to show the relationship between the previous work and the current study in order to determine the accuracy of the current work. An excellent concurrence is established by the comparison. Additionally, it is demonstrated that the application of N and Da improves fluid flow, respectively. The accuracy of the current analysis is confirmed by successfully recovering the work of Ojemeri and Onwubuya (2023c) by setting N and Da to be 0 and 1000, respectively, such that the term 1/Da vanishes.

Table 1: Showcases the numerical comparison of Ojemeri and Onwubuya's (2023c) work with the present study for velocity gradient for $\gamma = \Gamma = 1$, M = 1, when and Da. when $\mathbf{N = 0}$ and $\mathbf{Da = 1000}$.

Z	**Ojemeri and Onwubuya (2023c)** $\boldsymbol{\gamma = \Gamma = 1,}$ $\boldsymbol{\lambda = 0.001}$		**Present work** $\boldsymbol{\gamma = \Gamma = 1,}$ $\boldsymbol{\lambda = 0.001}$ $\mathbf{Da = 1000,}$ $\mathbf{N = 0}$		**Present work** $\mathbf{Da = 1, N = 1}$	**Present work** $\mathbf{Da = 1, N = 3}$
	θ (z)	U(z)	θ (z)	U(z)	U(z)	U(z)
0.1	0.4500	0.0843	0.4500	0.0843	0.1336	0.2830
0.2	0.4000	0.0856	0.4000	0.0856	0.1401	0.3012
0.3	0.3500	0.0831	0.3500	0.0831	0.1432	0.3150

0.4	0.3000	0.0772	0.3000	0.0772	0.1430	0.3232
0.5	0.2500	0.0686	0.2500	0.0686	0.1389	0.3234

5. Conclusion

Arrhenius-controlled heat transfer flow is studied in a magnetized free convection via a porous microchannel with SHO features to determine the effect of the nonlinearity variable. The novel ordinary differential equations governing the flow in terms of temperature and velocity components are derived using a semi-analytical (regular perturbation) method. Additionally, the physical aspects of engineering issues, such as shear stress and the Nusselt number, have also been calculated. Line graphs are used to illustrate the impact of the fluid's important parameters. These results are compared with earlier research for the limiting scenario (N=0, Da=1000), and there is extremely good concordance. Below is a summary of some intriguing findings from this paper:

(i) Nonlinear density with temperature (NDT) achieves a higher velocity than linear density with temperature (LDT).

(ii) The fluid velocity significantly increases with an increase in the Darcy porous parameter.

(iii) It is anticipated that λ will enhance the fluid's temperature and velocity gradients.

(iv) By increasing the temperature jump and velocity slip parameters, respectively, the fluid's temperature and velocity are at their maximum.

(v) It was determined that while a contrast behavior occurs at the plate (y = 1), greater values of the parameter N improve skin friction at the plate (y = 0).

(vi) For mounting level of M, the shear stress is greater at the surface (y = 0), whereas the opposite is true at (y = 1).

(vii) In the future, the effect of mixed convection would be studied on this model.

Appendix

$$M_1 = M^2 + \frac{1}{Da}, R_1 = -R_2, R_2 = \frac{1}{1+\Gamma}, R_3 = \frac{\left(\frac{1}{2}+\frac{R_1}{6}+\frac{R_2}{2}+e_1\frac{R_1^2}{12}+e_1\frac{R_1R_2}{3}+e_1\frac{R_2^2}{2}\right)}{1+\Gamma}, R_4 = \Gamma R_3$$

$$R_5 = \gamma[M_1R_6 + R_8] - R_9, R_6 = \frac{-\gamma R_8 cosh(M_1) + R_9 cosh(M_1) - e_2}{\gamma M cosh(M) + sinh(M)}, R_7 = \frac{NR_1^2}{M_1^2},$$

$$R_8 = \frac{R_1 + 2NR_1R_2}{M_1^2}, R_9 = \frac{R_2 + NR_2^2 + 2R_7}{M^2}, R_{10} = \gamma[M_1R_{11} + R_{16}] - R_{17},$$

$$R_{11} = \frac{-e_{10} - e_9}{\gamma M_1 cosh(M_1) + sinh(M_1)}, R_{12} = \frac{-e_3}{M_1^2}, R_{13} = \frac{-e_4}{M_1^2}, R_{14} = \frac{(e_3 + 20R_{12})}{M_1^2},$$

$$R_{15} = \frac{(e_6 + 12R_{13})}{M_1^2}, R_{16} = \frac{(e_7 + 6R_{14})}{M_1^2}, R_{17} = \frac{(e_8 + 2R_{15})}{M_1^2}, e_1 = \frac{1}{2} - \varepsilon,$$

$$e_2 = R_7 + R_8 + R_{9,}\, e_3 = \frac{2\mathrm{N}R_1^3 e_1}{12}\,, e_4 = \frac{R_1^2 e_1}{12} + \frac{2\mathrm{N}R_1^2}{6} + \frac{2\mathrm{N}R_1^2 R_2 e_1}{3} + \frac{2\mathrm{N}R_1^2 R_2 e_1}{12},$$

$$e_5 = \frac{R_1}{6} + \frac{R_1 R_2 e_1}{3} + \frac{2\mathrm{N}R_1}{2} + \frac{2\mathrm{N}R_1 R_2}{2} + \frac{2\mathrm{N}R_1 R_2^2 e_1}{2} + \frac{2\mathrm{N}R_1 R_2}{6} + \frac{2\mathrm{N}R_2^2 R_1 e_1}{3}$$

$$e_6 = \frac{1}{2} + \frac{R_2}{2} + \frac{R_2^2 e_1}{3} + 2\mathrm{N}R_1 R_3 + \mathrm{N}R_2 + \mathrm{N}R_2^2 + \frac{2\mathrm{N}R_2^3 e_1}{2}, e_7 = -R_3 - 2\mathrm{N}R_1 R_4 - 2\mathrm{N}R_2 R_3$$

$$e_8 = -R_4 - 2\mathrm{N}R_2 R_4, e_9 = R_{12} + R_{13} + R_{14} + R_{15} + R_{16} + R_{17}, e_{10} = (\gamma R_{16} - R_{17})cosh(M_1)$$

Nomenclature

B_0=constant magnetic flux density [kg/s^2.m^2]

g = force of gravity [m/s^2]

h= size of the channel [m]

M= magnetic parameter (-)

N= Nonlinear density variable with temperature (-)

Da = Darcy porous parameter (-)

ε = activation energy

T=nondimensional temperature of the fluid [K]

T_0=reference temperature [K]

u= nondimensional velocity of the fluid [ms^{-1}]

U_0=reference velocity [ms^{-1}]

Greek letters

γ = velocity slip parameter (-)

Γ = temperature jump parameter (-)

λ =chemical reacting parameter (-)

β =thermal expansion coefficient [K^{-1}]

μ =variable viscosity of the fluid [kgm^{-1}s^{-1}]

k=conductivity of the thermal fluid [m.kg/s^3.K]

α =thermal diffusivity[m^{2}s^{-1}]

σ = conductivity of the electrical fluid [s^{3}m^2/kg]

ρ = fluid's density [kgm^{-3}]

v =fluid's viscosity [m^2s^{-1}]

REFERENCES

Akhtari, M. R. and Karimi, N. (2020). Thermohydraulic analysis of a microchannel with varying superhydrophobic roughness, *Applied Thermal Engi*neering, 172, https://doi.org/10.1016/j.applithermaleng.2020.115147.

Hamza, M. M. (2016). Free convection slip flow of an exothermic fluid in a convectively heated vertical channel, *Ain Shams Engi*neering *Jour*nal, 9(4), http://dx.doi.org/10.1016/j.asej.2016.08.011.

Hamza, M. M., Ahmad, S. K., Ojemeri, G., Usman H. and Shuaibu, A. (2023b). Exploring the dynamics of an exothermic chemical reaction controlled by Arrhenius kinetics with Hall effect in a microchannel, *FUDMA Jour*nal of *Scie*nces, 7(3), 112-124.

Hamza, M. M., Balarabe A. Y., Ibrahim M., Akpootu D. O. and Sheriff A. (2025). Transient fractional dusty fluid flow in a superhydrophobic microchannel, *European Physical Journal Plus,*140, 366, 1-17.

Hamza, M. M., Ojemeri, G. and Ahmad, S. K. (2023a). Insights into an analytical simulation of a natural convection flow controlled by Arrhenius kinetics in a micro-channel, *Heliyon* 9(2023) e17628, 1-13.

Hamza, M. M., Shehu, A., Muhammad, I., Ojemeri, G., Shuaibu, A. (2024b). Electrokinetically controlled mixed convective heat flow in a slit microchannel, *Heat Transfer*, DOI:10.1002/htj.23104.

Hamza, M. M., Shehu, A., Muhammad, I., Shuaibu, A., Ojemeri, G. (2024a). Electro-kinetically free convective heat flow in a slit microchannel, *Inter*national *Jour*nal of *Applied Computatio*nal *Mathematics,* 10, https://doi.org/10.1007/s40819-024-01765-x.

Hartmann, J. and Lazarus F. (1937). Hg-dynamics II: theory of laminar flow of electrically conductive liquids in a homogeneous magnetic field, *Matematisk-Fysiske Meddelelser*, 15(7).

Heidarian, A., Rafee, R., Valipour, M. S. (2020). Effects of wall hydrophobicity on the thermohydraulic performance of the microchan nels with nanofluids, *Inter*national. *Communication in Heat Mass Transfer*, 117. https://doi.org/10.1016/j.icheatmasstransfer.2020.104758.

Jawad M., Saeed, A. and Gul T. (2021). Entropy generation for MHD Maxwell nanofluid flow past a porous and stretching surface with Dufour and Soret effects, *Brazilia*n *Jour*nal of *Physics*, pp. 1-13. htttps://doi.org/10.1007/s13538-020-00835.

Jha, B. K. and Gwandu, B. J. (2018). MHD free convection flow in a vertical slit micro-channel with super-hydrophobic slip and temperature jump: Heating by constant wall temperature, *Alexandria Engineering Journal,* 57, https://dx.doi.org/10.1016/j.aej.2017.08.022.

Jha, B. K. and Gwandu, B. J. (2019). MHD free convection flow in a vertical slit micro-channel with super-hydrophobic slip and temperature jump: non-linear Boussinesq approximation approach, *SN Applied Sciences,* DOI: 10.1007/S42452-019-0617-Y.

Jha, B. K. and Gwandu, B. J. (2020). MHD free convection flow in a vertical porous super-hydrophobic microchannel, *Journal of Process Mechanical Engineering*, 235 (2).

Jha, B. K., Altine, M. M. and Hussaini, A. M. (2023). MHD steady natural convection in a vertical porous channel in the presence of point/line heat source/sink: An exact solution, *Heat Transfer, Wiley,* pp. 1-15. DOI: 101002/htj.22903.

Lee, H., Fridlind A. M. and Ackerman, A. S. (2021). An evaluation of size-resolved cloud microphysics scheme numerics for use with radar observations, Part II: Condensation and Evaporation, *Journal of Atmospheric Sciences,* 78(5), 1629-1645. DOI:10.1175/JAS-D-20-0213.1.

Obalalu, A. M., Ajala, O. A., Adeosun, A. T., Akindele, A. O., Oladapo, O. A., Olajide, O. A., (2021). Significance of variable electrical conductivity on non-Newtonian fluid flow between two vertical plates in the coexistence of Arrhenius energy and exothermic chemical reaction, *Partial Differe*ntial *Equatio*n *a*nd *Applied Mathematics,* 4, 1-9. 100184.

Ojemeri, G. and Hamza, M. M. (2022). Heat transfer analysis of Arrhenius-controlled free convective hydromagnetic flow with heat generation/absorption effect in a micro-channel, *Alexandria Engineering Journal*, **61**, 12797-12811.

Ojemeri, G. and Onwubuya, I. O. (2023a). Exploring the dynamics of viscous dissipative fluid past a super-hydrophobic microchannel in the coexistence of mixed convection and porous medium*, Saudi J. Eng. Tech*, 8, 71-80.

Ojemeri, G. and Onwubuya, I. O. (2023b). Analysis of mixed convection flow on Arrhenius-controlled heat generating/absorbing fluid in a superhydrophobic microchannel: A semi-analytical approach, *Dutse Journal of Pure and Applied Sciences,* 9a**,** 344-357.

Ojemeri G. and Onwubuya, I. O. (2023c). Investigation of Arrhenius-controlled chemical reaction through a superhydrophobic microchannel, *FUDMA Jour*nal *of Scie*nces*,* 7(3), 80-86.

Ojemeri, G., Omokhuale, E., Hamza, M. M., Onwubuya, I. O., Shuaibu, A. (2023a). A Computational Analysis on Steady MHD Casson Fluid Flow Across a Vertical Porous Channel Affected by Thermal Radiation Effect*, International Journal of Sciences and Global Sustainabilty,* **9**(1). https://doi.org/ 10.57233/ijsgs.v9i1.393.

Ojemeri, G., Onwubuya, I. O., Shuaibu, A., Omokhuale, E. and Altine, M. M. (2023b). Arrhenius-controlled heat transfer fluid provoked by porosity effect through a vertical microchannel: An analytical approach, *Continental Journal of Applied Sciences,* 18(1), 18-40.

Ojemeri, G., Onwubuya, I. O., Omokhuale, E., Hussaini A. and Shuaibu, A. (2024). Analytical investigation of Arrhenius kinetics with heat source/sink impacts along a heated superhydrophobic microchannel, *UMYU Scientifica,* 3(1), pp 61-71. DOI:105619/usci.2431.004.

Onwubuya, I. O. and Ojemeri, G. (2023). Evaluation of mixed convection-radiation flow of a viscous fluid restricted to a vertical porous channel: A comparative Study, *Caliphate Journal Science and Technology*, 5(3), 1-9.

Reddy, J. V. R., Kumar, K. A., Sugunamma, V., Sandeep, N. (2018). Effect of cross diffusion on MHD non-Newtonian fluids flow past a stretching sheet with non-uniform heat source/sink: A comparative study, *Alexandria Engineering Journal,* **57**(3), 1829–1838.

Rostami, H T., Fallah, N. M., Hosseinzadeh, Kh. and Ganji, D. D. (2021). Investigation of mixture-based dusty hybrid nanofluid flow in porous media affected by magnetic field using RBF method, *Inter*national *Jour*nal *of Ambie*nt *Energy.* DOI: 10.1080/01430750.2021.20230.

Saeed, A. and Gul, T. (2021). Bio-convection Casson nano-fluid flow together with Darcy-Forchheimer due to a rotating disk with thermal radiation and Arrhenius activation energy, *SN Applied Science*, **3**, 78.

Sharma, H., Gaddam, A., Agrawal, A., Joshi, S.S. and Dimov, S. S. (2020). Influence of texture shape and arrangement on thermo-hydraulic performance of textured microchannels, *Inter*national *Jour*nal *of Thermal Sci*ences, 147. https://doi.org/10.1016/j.ijthermalsci.2019.106146,

Sia, G. D., Lim, C.S., Tan, M. K., Chen, G. M. and Hung, Y. M. (2023). Anomalously enhanced subcooled flow boiling in superhydrophobic graphene-nanoplatelets'-coated microchannels, *Inter*national *Commu*nication in *Heat a*nd *Mass Transfer,* 146, https://doi.org/10.1016/j.icheatmasstransfer.2023.106932.

Sravanthi, C. S. and Gorla, R. S. R. (2018). Effects of heat source/sink and chemical reaction on MHD Maxwell nanofluid flow over a convectively heated exponentially stretching sheet using Homotopy analysis method, *International Journal of Applied Mechanics and Engineering,* 23(1), 137–159.

Uygun, N. and Ahmad, H. T. (2022). The effect of Hall parameter on the MHD fluid flow and heat transfer induced by uniform radial electric field due to a shrinking rotating disk, *Case Studies i*n *Thermal Engineering,* 37, 102222.

Zhang, W., Wang, Zeng M. and Zhao, C. (2019). Thermoelectric effect and temperature-gradient-driven electrokinetic flow of electrolyte solutions in charged nanocapillaries*, Inter*national *Jour*nal of *Heat a*nd *Mass Transfer,* 143. *https://*doi:10.1016/j.ijheatmasstransfer.2019.118569.